# Influence of *in situ* ultrasound treatment during ion implantation on amorphization and junction formation in silicon

D. Krüger
*IHP, Frankfurt (Oder), Im Technologiepark 25, 15236 Frankfurt (Oder), Germany*

B. Romanyuk, V. Melnik, and Ya. Olikh
*Institute for Semiconductor Physics of the Ukrainian Academy of Science, Prospekt Nauki 45, 252028 Kiev, Ukraine*

R. Kurps
*IHP, Frankfurt (Oder), Im Technologiepark 25, 15236 Frankfurt (Oder), Germany*

(Received 28 September 2001; accepted 20 May 2002)

We report the first study of the effect of *in situ* ultrasound treatment during ion implantation on amorphization and transient enhanced diffusion (TED) in silicon. Rutherford backscattering spectroscopy, ion channeling, and Raman spectroscopy measurements show that amorphization of Si during Ar ion implantation is increased by ultrasound treatment, especially at ultrasound frequencies around 2 MHz. By secondary ion mass spectroscopy we investigate the influence of ultrasound treatment on TED of B atoms. Our data show that TED is reduced due to the influence of ultrasound treatment. The results are discussed in terms of the interaction of ultrasound waves with point defects and the ultrasound stimulated enhanced diffusion of interstitials.  [DOI: 10.1116/1.1493784]

## I. INTRODUCTION

Following the *SIA Roadmap*, the fabrication of advanced electronic devices in complementary metal–oxide–semiconductor (CMOS) and BiCMOS technologies requires a reduction of the *pn*-junction depth below 30 nm for the year 2005. Conventional ion implantation is faced with several challenges to stay in line with the Roadmap. Increased implantation doses and increased dopant activation are critical to maintain low sheet resistance. Moreover, creating ultra-shallow junctions by ion implantation, several processes limit the junction depth, such as: (i) ion channeling during implantation; (ii) transient enhanced diffusion (TED), see, e.g., Ref. 1; and (iii) formation of clusters, see, e.g., Ref. 2. Transient enhanced diffusion, as known, is mainly related due to high nonequilibrium silicon interstitial concentrations. It was shown in Refs. 3 and 4 that TED can be suppressed by carbon incorporation into silicon reducing the excess interstitial concentration.

Ion implantation induced amorphization is widely used to reduce channeling tails of dopant profiles. Amorphization also influences the type and concentration of defects remaining after subsequent thermal annealing. Several theoretical models have been proposed to describe aspects of the amorphization process, such as the overlap of damaged regions, the out-diffusion of point defects, and the deposited energy density (e.g., Refs. 5 and 6). Despite numerous studies, a detailed understanding of the crystalline–amorphous phase transformation is still not available.

It has been suggested that ultrasound waves propagating through the semiconductor can affect the generation of point defects and cause, e.g., dissociation of defect complexes.[7] Ostapenko *et al.* found that ultrasound treatment (UST) enhances the dissociation of FeB pairs in poly-Si, and increases the diffusion length of minority carriers.[8] Recently, a review on ultrasound stimulated processes in semiconductors was published.[9] From our point of view, it seems promising to use UST *in situ*, i.e., during the implantation process, while the target atoms are still in an excited state and defect complexes are unstable or highly metastable.

Here, we report on the *in situ* modification of the implantation process in Si by ultrasound. We show that the defect density in the surface layer and the thickness of the amorphous layer increase by UST. We observe a suppression of boron TED in silicon due to the influence of UST. We explain the results through an interaction of ultrasound with point defects, taking into account enhanced diffusion of interstitials, decreasing point defects recombination, and UST stimulated formation of vacancy complexes.

## II. EXPERIMENT

(100) boron-doped, CZ–Si samples ($\rho = 10\ \Omega$ cm) were mounted inside the implantation chamber on piezoelectric transducers via acoustics binders. Low amplitude ultrasound vibrations were generated in the wafer by operating the transducer in a resonance vibration mode. The basic resonance frequency was varied from 600 kHz to 7 MHz. The amplitude of the generated deformation did not exceed $10^{-5}$ of the lattice constant corresponding to an acoustic power of $1\ \mathrm{W\,cm^{-2}}$. For implantation we used ions of different mass ($^{40}Ar^{+}$, $^{28}Si^{+}$, and $^{11}B^{+}$) with energies from 50 to 150 keV and doses between $1\times10^{13}$ and $1\times10^{16}\ \mathrm{cm^{-2}}$. The ion flux was varied from $6\times10^{10}$ to $3\times10^{12}\ \mathrm{cm^{-2}\,s^{-1}}$. We also implanted $^{28}Si^{+}$ ions ($D = 3\times10^{14}\ \mathrm{cm^{-2}}$, $E = 125$ keV) into a doping superlattice (DSL) of equidistant (100 nm) B spikes,

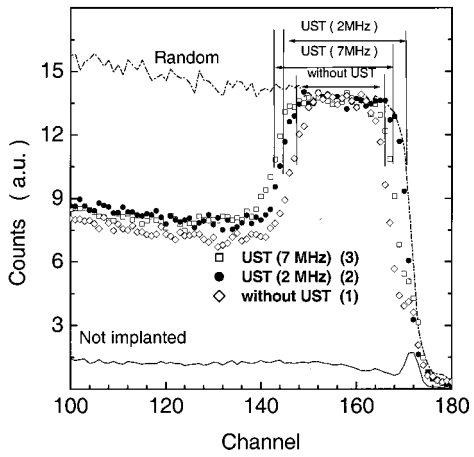


FIG. 1. 1.5 MeV He ions RBS channeling spectra of (100) Si samples implanted with Ar ions at a dose of $4\times10^{14}$ cm$^{-2}$. Indicated spectra for implantation without UST and with UST at $f_{UST}=2$ MHz and $f_{UST}=7$ MHz, respectively. For comparison a random spectrum and the channeling spectrum of an untreated crystal are shown.

grown by molecular beam epitaxy (MBE). The maximum of the implanted $^{28}Si^+$ peak was located at a depth of about 200 nm, near the second B spike in the B-DSL.

Damage accumulation was monitored by Rutherford backscattering (RBS) and channeling (RBS-C) using 1.5 MeV He ions at a scattering angle of 170°.

The implanted structures were studied by Raman spectroscopy (RS) with the spectra excited by an Ar laser (514.5 nm). To obtain more detailed information about the disordered layers the implanted structures were also studied by multiangle spectral ellipsometry in the spectral range from 225 to 1200 nm using incidence angles from 60° to 80°.

TED was investigated in samples after post-implantation annealing at 900 °C for 30 s. Boron depth profiles were measured by secondary ion mass spectrometry (SIMS) using an ion microprobe ATOMIKA 6500 with mass-filtered $O_2^+$ ions at different energies from 3 to 9 keV at normal incidence.

## III. RESULTS

Figure 1 shows RBS-C spectra for samples implanted with 150 keV $Ar^+$ at 20 °C to a total dose of $4\times10^{14}$ cm$^{-2}$. The samples were implanted without an ultrasound transducer (1), or with ultrasound transducers with resonance frequencies of 2 (2) and 7 MHz (3), respectively. The use of ultrasound transducers increases the amount of damage. A movement of both crystalline–amorphous ($c-a$) interfaces was observed by cross-sectional TEM (not shown). Correspondingly, the thickness of the amorphous layer is larger in the ultrasound treated samples in agreement with the RBS-C results. In wafers implanted without UST a buried amorphous layer is formed and a crystalline layer at the surface remains. On the contrary, a continuous amorphous layer up to the surface is formed in samples with UST (2 MHz). For ultrasound frequencies $f_{UST}=7$ MHz only small displacements (about 20 nm, according to TEM data) of the inner $a-c$ interface towards the Si bulk are observed. For comparison Fig. 1 also shows the random and channeling spectra for an untreated sample.

The thickness of the characteristic layers obtained from RBS and ellipsometric data for different samples are presented in Table I. In ellipsometry, the measured parameters are the ellipsometric angles $\Psi$ and $\Delta$ describing relative changes of amplitude and phase between different conditions of polarization. The layer parameters were determined by simulation using a least square fit. The ellipsometric data (see Table I) confirm the results of an increased amorphized layer thickness, obtained from the RBS spectra.

Raman spectra for Si samples implanted with $Ar^+$ ions under UST with different frequencies are presented in Fig. 2. We note maxima located at 521 and 480 cm$^{-1}$ originating from the crystalline and amorphous phases, respectively. These maxima correspond to phonon scattering near the center of the Brillouin zone in the crystalline phase (peak at 521 cm$^{-1}$) and to scattering on phonons with random wave vectors in the amorphous phase in the region of $\sim$480 cm$^{-1}$.[10] By comparison of the spectra we conclude

TABLE I. Thickness of buried amorphous and near-surface crystalline layers as obtained from RBS and ellipsometry measurements after 150 keV $Ar^+$ implantation at 20 °C ($D=4\times10^{14}$ cm$^{-2}$).

| Method | Layers | Thickness of the disordered layers (with UST, $f_{UST}=2$ MHz) | Thickness of the disordered layers (without UST) |
|---|---|---|---|
| RBS | 1 | *a*-Si | *a*-Si+*c*-Si |
| | 2 | *a*-Si+*c*-Si | *a*-Si |
| | 3 | *c*-Si(substrate) | *a*-Si+*c*-Si |
| | 4 | | *c*-Si(substrate) |
| | | Total-224 nm | Total-176 nm |
| Ellipsometry | 1 | Surface $SiO_2$-5.37 nm | Surface $SiO_2$-6.48 nm |
| | 2 | *a*-Si+8.7% voids-59.74 nm | *c*-Si+41.2% *a*-Si-17.76 nm |
| | 3 | *a*-Si+16.1% voids-55.03 nm | *a*-Si-74.88 nm |
| | 4 | *a*-Si+34.5% voids-145.39 nm | *a*-Si+22% voids-134.69 nm |
| | 5 | *c*-Si+45.6% *a*-Si+14.9% voids-87.03 nm | *c*-Si(substrate) |
| | 6 | *c*-Si(substrate) | |
| | | Total-347 nm | Total-228 nm |

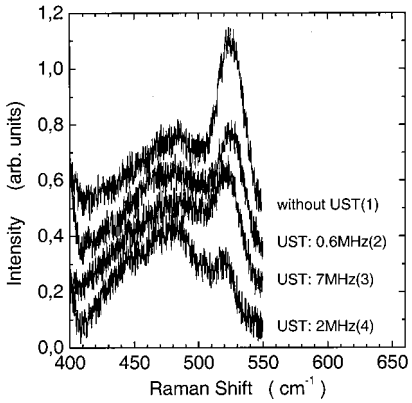


FIG. 2. Raman spectra from as-implanted Si samples (150 keV $Ar^+$, $4\times10^{14}$ cm$^{-2}$) without UST, with UST at $f_{UST}=0.6$ MHz, with UST at $f_{UST}=7$ MHz, and with UST at $f_{UST}=2$ MHz.

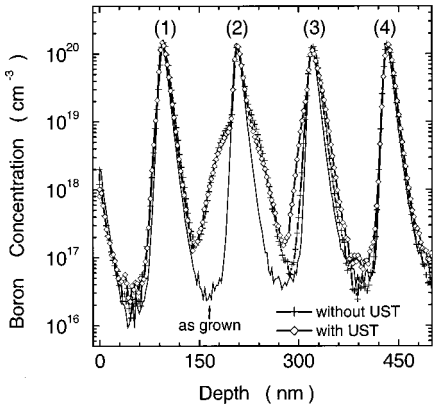


FIG. 4. SIMS profiles of B-DSLs implanted with $^{28}Si^+$ ions ($D=3\times10^{14}$ cm$^{-2}$, $E=125$ keV) after annealing at 820 °C for 30 s. The as-grown profile is compared with the samples implanted with and without UST. The four B spikes in the DSL are marked.

that UST leads to a decrease of the crystalline fraction and to an increase of the amorphous one. The most effective influence on the amorphization process is obtained with an ultrasound transducer at a frequency of $f_{UST}=2$ MHz. Additionally, we find a shift of the maximum at 521 cm$^{-1}$ towards lower energies caused by tensile strain (about $5.5\times10^8$ N m$^{-2}$) for $f_{UST}=2$ MHz. In samples without UST compressive strain is detectable.

For implantation conditions that do not result in amorphization, e.g., in case of implantation with light atoms, such as B defect concentrations after annealing are lower for wafers implanted with ultrasound treatment compared to reference wafers implanted without ultrasound treatment. This we proved by etching experiments and TEM analysis (not shown).

SIMS results for the samples implanted with B (dose $3\times10^{14}$ cm$^{-2}$) are presented in Fig. 3. After annealing at 900 °C for 30 s, the B profile at a concentration level of $2\times10^{17}$ cm$^{-3}$ is shifted by about 100 nm compared to the sample implanted without UST. This shift is related mostly to TED. UST significantly changes the resulting B profile. The corresponding B profile reveals only a small shift (about 20 nm) from the as-implanted one. Additionally, a small shift of the concentration maximum towards the surface (20 nm) is observed. These results show that TED of B can be suppressed by UST.

Figure 4 shows SIMS depth profiles for a B-DSL sample implanted by $^{28}Si^+$ with and without UST. The maximum of the implanted $^{28}Si^+$ peak was located near the second B spike in the B-DSL (2). TED effects are clearly visible near the Si peak, both for the samples implanted with and without UST after an annealing at 820 °C for 30 s. At the same time, an additional spike smearing effect for the sample implanted with UST occurs in the depth region of the third B spike (3). We conclude that an excess interstitial concentration due to the influence of UST is present in this depth region.

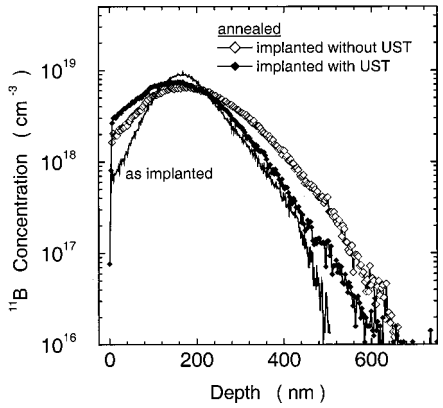


FIG. 3. SIMS profiles from Si wafers implanted with $B^+$ ions ($D=2.2\times10^{14}$ cm$^{-2}$, $E=40$ keV) with UST ($f_{UST}=7$ MHz) and without UST after annealing at 900 °C for 30 s. For comparison the as-implanted profile is shown.

## IV. DISCUSSION

We propose that ultrasound induced enhanced amorphization can be modeled in terms of ultrasound stimulated diffusion of interstitials, decreased point defects recombination, and kinetic changes in vacancy complexes formation. In case of $Ar^+$ implantation, every ion creates a disordered area with a diameter of about 3 to 6 nm.[11] Subsequently, cascade cooling, partial recombination of point defects, and creation of point defect complexes take place. If the implantation dose increases, amorphous areas are created, which grow by absorption of point defects. Finally, they overlap, forming a continuous amorphous layer.

The presence of ultrasound waves with a moderate intensity (0.1 to 1.0 W/cm$^2$) over the frequency 0.6–7 MHz in the crystal lattice generates substantially less energy compared to that deposited in the lattice by the incident ion beam. Therefore, in absence of ion irradiation we could not detect any changes in the crystal from the sound field alone. However, our experiments prove that *in situ* ultrasound excitation during ion implantation increases the amorphized layer thickness (Fig. 1, Table I) and therefore reduces the critical

amorphization dose. Table I shows differences in total thickness of the disordered layer obtained from RBS and ellipsometry. The observed results can be explained by the presence of slightly disordered regions, modifying the optical constants. Such areas are well distinguished by ellipsometry but are not fixed by RBS. UST at 2 MHz results in a movement of the outer $a-c$ interface towards the surface, where usually vacant defects are accumulated. We assume, in analogy with ultrasound gas bubbles cavitation in liquids,[12] that during implantation UST stimulates the following processes: (i) coupling of vacancies into complexes; (ii) tension compression of ''vacancy bubbles'' under ultrasound waves resulting in their deformation, growth, and movement to the surface; and (iii) formation of Ar bubbles. These processes enhance the overlap of disordered regions and stimulate the formation of a continuous amorphous layer up to the surface. An influence of UST on point defect and diffusion was also predicted in Ref. 13.

We assume that ultrasound at low frequencies (e.g., below 2 MHz) mainly influences the formation of large vacancy complexes, which are located near the surface. Raman measurements reveal tensile strain in this region, connected with increasing vacancy concentration. Ultrasound at higher frequencies (e.g., above 7 MHz) seems to mainly influence point defect diffusion. Absorption of phonons generated by the ultrasound wave with frequencies in the range 0.6–7 MHz by the lattice will lead only to a small decrease of the activation energy of diffusion. However, low frequency ultrasound can also excite high frequency phonons as a result of nonlinear processes.[12] Absorption of these phonons seems to be important for diffusion enhancement. Moreover, in the frequency range used, the wavelength of ultrasound equals approximately the sample thickness. Periodic tensile and compressive strain leads to a gradient of mechanical strain in the direction of the ion beam. As a result, an increased interstitial flow towards the bulk of the wafer is generated by the strain gradient compared to the flow directed toward the surface. The implanted boron atoms create barriers for Si interstitial diffusion toward the surface.

As shown above, TED of ion implanted B is suppressed in the presence of UST during implantation. We suggest, that this effect is related to UST stimulated diffusion of Si interstitials from the implanted depth region towards the bulk of wafer. Therefore, the formation of mobile B interstitial complexes, responsible for enhanced B diffusion, is also suppressed. This hypothesis is supported by our experiments of $Si^+$ implantation into B-DSLs. The excess broadening of the third B spikes (3) in Fig. 4 is related to increased Si interstitial concentration in this depth region. The effect takes place only in samples implanted with *in situ* UST. Therefore, we conclude the existence of a UST induced interstitial migration of several 100 nm into the bulk of the wafer. A detailed analysis of the second spike (2) shows a slightly decreased broadening of this spike after UST.

Figure 3 reveals a shift of the boron profile toward the surface in samples implanted with UST. This shift is a result of boron diffusion toward the surface during annealing where an excess vacancy concentration can be assumed.

## V. SUMMARY

We have investigated for the first time the effect of *in situ* ultrasound treatment during ion implantation on amorphization and transient enhanced diffusion in silicon. Appropriate ultrasound treatment enhances amorphization of Si during Ar implantation, especially at lower frequencies (below 2 MHz). The effect depends on ion flux, ultrasound frequencies, and ion masses. In the case of implantation of light atoms, the defect concentration after annealing is lower for wafers implanted with ultrasound treatment compared to reference samples. Suppressed boron transient enhanced diffusion was found in the case of ultrasound treatment during implantation. Therefore, ultrasound treatment can be used for the reduction of B diffusion in application of ultra-shallow junction formation. The experimentally observed effects are discussed in terms of ultrasound stimulated enhanced point defect diffusion, interaction, and clustering. Ultrasound treatment stimulated diffusion of excess Si interstitials from the implanted depth region towards the bulk of wafer reduces transient enhanced diffusion of B.

## ACKNOWLEDGMENTS

This article was supported by the BMBF project 01 M 2976. The authors greatly appreciate the support of V. Yuchimchuk and A. Franzkevich. We thank Professor A. Ourmazd and Dr. K. Pressel for helpful discussions.

Presented at the Sixth International Workshop on Fabrication, Characterization, and Modeling of Ultra-Shallow Doping Profiles in Semiconductors (USJ2001), 22–26 April 2001, Napa, CA.

[1]P. A. Stolk, J. H. I. Cossman, D. J. Eaglesham, D. C. Jacobson, C. S. Rafferty, G. H. Gilmer, M. Jariz, and J. M. Poate, J. Appl. Phys. **81**, 6031 (1997).
[2]S. Solmi, M. Bersani, M. Sbetti, J. Lundsgaard Honsen, and A. Nylandsted Larsen, J. Appl. Phys. **88**, 4547 (2000).
[3]N. E. B. Cowern, A. Caccianto, J. S. Custer, F. W. Saris, and W. Vandervost, Appl. Phys. Lett. **76**, 855 (2000).
[4]H. Rücker, B. Heinemann, D. Bolze, D. Knoll, D. Krüger, R. Kurps, H.-J. Osten, P. Schley, B. Tillack, and P. Zaumseil, Tech. Dig. - Int. Electron Devices Meet. **1999**, 345 (1999).
[5]J. R. Dennis and E. B. Hale, J. Appl. Phys. **49**, 1119 (1978).
[6]J. F. Gibbons, Proc. IEEE **60**, 1062 (1972).
[7]I. V. Ostrovskij and V. N. Lisenko, Sov. Phys. Solid State **24**, 682 (1982).
[8]S. Ostapenko, L. Jastrebskij, and B. Sopori, Semicond. Sci. Technol. **10**, 1494 (1995).
[9]S. Ostapenko, Appl. Phys. A: Solids Surf. **69**, 225 (1999).
[10]Landolt–Börnstein, *Neue Serie*, Gruppe III, Vol. 17, p. 390.
[11]G. Götz, E. Glaser, W. Wesch, and N. Sobolev, Proceedings of the International Conference on Radiative Physics of Semiconductors, Tbilisi, 1982, p. 391.
[12]*Current Trends in Sonochemistry*, edited by C. J. Price (Royal Society of Chemistry, London, 1982).
[13]V. Arakelyan and A. Avakyan, Phys. Status Solidi A **80**, K71 (1983).